

A unified approach of energy and data cooperation in energy harvesting WSNs

Roomana YOUSAF^{1*}, Rizwan AHMAD¹, Waqas AHMED² & Fu-chun ZHENG³

¹*School of Electrical Engineering and Computer Science, National University of Sciences and Technology, Islamabad 44000, Pakistan;*

²*Department of Electrical Engineering, Pakistan Institute of Engineering and Applied Sciences, Islamabad 44000, Pakistan;*

³*School of Electronic and Information Engineering, Harbin Institute of Technology, Shenzhen 518055, China*

Received 30 March 2017/Revised 24 July 2017/Accepted 31 August 2017/Published online 18 May 2018

Abstract Energy harvesting (EH) provisioned wireless sensor nodes are key enablers to increase network life time in modern wireless sensor networks (WSNs). However, the intermittent nature of the EH process necessitates management of nodes' limited data and energy buffer capacity. In this paper, a unified mathematical model for a cooperative EHWSN with an opportunistic relay is presented. The energy and data causality constraints are expressed in terms of throughput, available energy, delay and transmission time. Considering finite energy buffers, data buffers and discrete transmission rates (as defined in the standard IEEE 802.15.4) at the nodes, different intuitive online power allocation policies at the relay are studied. The results show that a policy achieving high throughput is less fair and vice versa. Therefore, a joint rate and power allocation policy (JRPAP) is proposed in this study which provides a better trade off between fairness, throughput and energy over intuitive policies. Based on the JRPAP results, we propose to use data aggregation (DA) to achieve throughput gain at lower buffer sizes. In addition, the notion of energy aggregation (EA) is introduced to achieve throughput gain at higher buffer sizes. Combining both EA and DA further improves the overall throughput at all buffer sizes.

Keywords energy harvesting, energy causality, data causality, energy aggregation, data aggregation, opportunistic relay

Citation Yousaf R, Ahmad R, Ahmed W, et al. A unified approach of energy and data cooperation in energy harvesting WSNs. *Sci China Inf Sci*, 2018, 61(8): 082303, <https://doi.org/10.1007/s11432-017-9257-1>

1 Introduction

In recent years, the demand for wireless sensors has increased manifold due to their usefulness in critical applications like healthcare, agriculture, environmental monitoring, smart metering and sensor clouds. This rapid deployment and advent of new technologies like internet of things (IoT) introduce complex sensor network topologies that requires extensive cooperation among nodes. This cooperation leads to higher energy consumption and it is difficult for the standard battery powered wireless sensor nodes to meet the performance demands of throughput, delay, transmission time and simultaneously provide lifelong operation unattended. Energy harvesting (EH) technology makes it possible for wireless sensors to overcome these drawbacks by enabling the nodes to replenish energy from the environmental sources [1]. On the other hand, the variations in environmental conditions cause fluctuations in EH levels. Therefore,

* Corresponding author (email: 12mseeryousaf@seecs.edu.pk)

energy harvesting wireless sensor networks (EHWSNs) have to schedule the transmissions only when enough energy is available which may compromise throughput.

In a cooperative EHWSN in which both the source and relay are EH nodes, the problem of maintaining throughput becomes more complex. Recently, a lot of research have been carried out to analyze and improve the throughput of cooperative EHWSNs. These studies can be categorized based on their assumptions of EH profile and causality, energy policy (offline and online), energy buffer size, data buffer size, data rates. For example, with the assumptions of infinite battery and offline knowledge of EH profile, the throughput maximization problem has been studied in [2–4]. Introducing the constraint of a limited battery capacity, the authors in [5] have studied the throughput in a two way relay channel with stochastic data arrival, finite energy and data storage using decode and forward relay scheme. However, this model assumes deterministic offline EH profile which may not be available all the time. For similar network settings, the impact of changing the size of data and energy buffers at the two transmitting nodes on throughput is studied in [6].

In EHWSNs the causality constraints and the environmental factors can significantly change the available energy. This dependence can be reduced by using energy cooperation or wireless energy transfer [7]. Two basic techniques that can be used for energy transfer are inductive coupling and electromagnetic (EM) radiation [8]. This energy cooperation can be augmented by data transfer as mentioned in [9]. The source node's capability to transfer energy along with data will help in improving the overall system performance. Networks consisting of nodes that are capable of both scavenging energy from surroundings and wireless charging can have significant increase in their network lifetime and throughput. Performance analysis in terms of power and transmission outage based upon simultaneous data and power transfer using RF signal is done in [10]. Authors in [11] have studied the performance analysis of clustered EHWSN in terms of energy efficiency using optimal power splitting ratio at the receiver and transmitter. The authors in [7] show that the nodes in a two-hop relay network can use energy transfer and harvesting technology to improve overall throughput. However, they have not considered the limited data buffer capacity at the relay node.

Extending the analysis, the authors in [12] have considered a network scenario consisting of multiple source destination pairs communicating through EH relay node. Outage probabilities for all the contending users are calculated under the assumptions of unlimited battery and buffer capacity. Throughput analysis of a two-hop network using different relaying schemes is studied in [13] with relay node capable of EH from the RF signal transmitted by the source node. Authors in [14] using finite battery and fixed slot length have shown the comparison of throughput gain with and without energy cooperation. In [15], different power allocation policies are proposed for EH relay network with relay nodes also capable of energy cooperation among themselves.

In aforementioned previous works, the effect of energy allocation policies and transmission scheduling techniques to improve the network performance for a given/assumed EH profile using different network parameters is studied. However, very limited research, particularly in EHWSN, has been focused on using realistic network parameters like discrete transmission rates, finite energy and data buffer capacity to improve network throughput. Thus further study is required to meet the challenges caused by the introduction of these realistic network parameters. This paper considers a cooperative EHWSN using opportunistic relay with finite energy and data buffer. The source node's data transmission is constrained with the available size of the forwarding buffer of the relay node in order to avoid data overflow. Unlike previous works [2–15], throughput analysis considers the overall network throughput. The main differentiating contributions of this paper are given as follows.

- It mathematically presents a unified energy and data cooperation model using opportunistic relaying. The proposed system model incorporates discrete data rates as specified by the standard for wireless sensor networks (WSNs) and realistic parameters such as, finite data buffer and energy buffer capacities at source and relay. The impact of energy cooperation based on energy transfer efficiency, multiple energy harvesting arrivals at source and relay nodes and no prior information about the EH profile is analyzed.
- It applies different power allocation policies proposed in literature to study the throughput, delay and energy response of the network. An improved joint rate and power allocation policy (JRPAP) is also

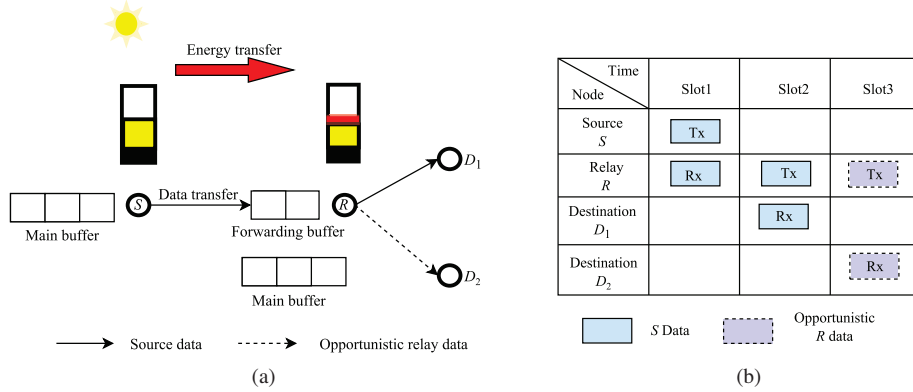


Figure 1 (Color online) (a) System model of an EHWSN; (b) time slot diagram of EHWSN.

proposed. The impact of this policy on transmission time, energy consumption, throughput, fairness and delay is also studied and compared with the intuitive policies.

- Opportunistic nature of the relay and its impact on overall throughput are analyzed by using energy and data aggregation.

The rest of the paper is organized as follows. In Section 2, system model with all the network constraints is presented. Section 3 describes the power allocation strategies at the relay node using the constraints mentioned in Section 2. It further presents a JRPAP at the relay node. Section 4 presents simulation results to demonstrate our solution. Finally, Section 5 concludes the paper.

2 System model

We consider an half-duplex additive white Gaussian noise (AWGN) channel with constant pathloss and four nodes: source S , relay R , and destinations D_1 (of source data) and D_2 (of relay data), as depicted in Figure 1(a). The transmitting nodes in the network are able to harvest energy and have finite data and energy buffers. The channel gains (path loss) between $S \rightarrow R$, $R \rightarrow D_1$ and $R \rightarrow D_2$ are represented by $h_{r,s}$, h_{r,d_1} and h_{r,d_2} , respectively. It is assumed that direct transmission between $S \rightarrow D_1$ is in outage due to high path loss (poor SNR). Similar to [16], the R node consists of one energy buffer and two data buffers, namely, main buffer and forwarding buffer as seen in Figure 1(a). The main buffer is used for the opportunistic transmission $R \rightarrow D_2$ and forwarding buffer is used for the source transmission $R \rightarrow D_1$. The maximum capacity of the forwarding buffer at R is denoted $BC_{r,max}$. The R node receives data from the S node and forwards it to D_1 . The S node can also hear this broadcast which will be used as acknowledgment that its data is delivered to D_1 .

The R node after successfully transmitting the S data acts opportunistically in the next slot, to transmit its own data, given enough energy is available as shown in Figure 1(b). At the end of an opportunistic transmission $R \rightarrow D_2$, the S node acquires the next transmission slot to forward its data to the R node. We assume that the R node will not accept any new data unless it has transmitted the data received in previous cycle(s). In this paper, only the energy required for transmission is considered [2, 17].

The S and R nodes are capable of energy cooperation (the process where the node can receive energy from another node within the network) with the help of energy transfer unit. The S node can transfer some portion of its energy to make the data cooperation between S and R successful. As the energy buffer is limited, it is in the interest of the S node to transfer its energy because it can harvest more energy in the coming EH instances. In addition to that, if it already has some stored energy then a portion of the new harvested energy is certainly lost resulting in a buffer overflow.

For data transmission, the energy causality constraint needs to be satisfied for both the nodes, which implies that the energy harvested in future EH intervals is not available for current transmission or for energy transfer. The time instance at which the node harvests energy is termed as EH instance. Energy harvested at each EH instance is saved in the energy buffer of the harvesting nodes. An online discrete

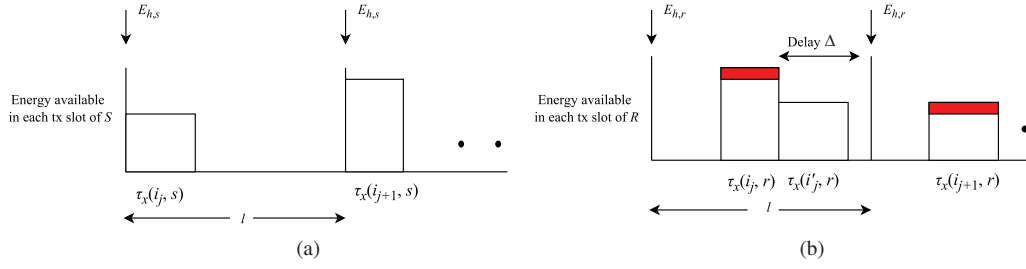


Figure 2 (Color online) Energy arrival and data transmission at (a) source, (b) relay.

time EH profile is considered which means that the harvesting node does not have the information of future energy arrival profile. The time between two energy arrivals is called an EH interval [18]. Energy arriving in any particular interval is available immediately for use as shown in Figure 2. If the available energy is less than what is required for successful transmission, the network nodes will wait for next EH instance to make their transmission successful. The transmitting nodes are capable of changing its rate based upon the available energy. A total transmission duration of T and L EH intervals are used for transmitting M_s amount of data bits from the $S \rightarrow D_1$ via R . The amount of energy harvested E_h by S and R nodes is denoted as $E_{h,s}$ and $E_{h,r}$, respectively. The length of EH interval is represented by l . At the start of an EH interval the energy available at S and R nodes is stored in the batteries of maximum capacity $E_{s,max}$ and $E_{r,max}$, respectively. The energy transferred to the R node depends upon the energy transfer efficiency coefficient $0 < \alpha \leq 1$. Let δ be the amount of energy transferred to the R node then $\alpha\delta$ amount of energy is received by the energy buffer. With the assumption that the channels are static, the value of α remains the same for complete transmission. During the EH process, at the start of each j -th interval with $j = \{1, \dots, L\}$ the amount of energies available at S and R nodes are $E_{ava,s}(j)$, $E_{ava,r}(j)$, respectively and is given as follows:

$$E_{ava,s}(j) = E_{h,s}(j) + E_{ava,s}(j-1), \quad (1)$$

$$E_{ava,r}(j) = E_{h,r}(j) + E_{ava,r}(j-1), \quad (2)$$

During the j -th EH interval, the i -th transmission slot is represented by i_j and the amount of energy available during the i_j slot is denoted by $E_{ava,s}(i_{j,s})$, $E_{ava,r}(i_{j,r})$, respectively where $i_j = \{1, \dots, N_j\}$ representing variable number of transmission slots within an EH interval. The indexing variables for transmission slots are given as $i_{j,s}$, $i_{j,r}$ and $i'_{j,r}$ such that $\{i_{j,s} \cup i_{j,r} \cup i'_{j,r} \in i_j\}$, $i_{j,s} \neq i_{j,r} \neq i'_{j,r}$. During an EH interval, $i_{j,s}$, $i_{j,r}$ and $i'_{j,r}$ are the transmission slots assigned for $S \rightarrow R$, $R \rightarrow D_1$ and $R \rightarrow D_2$ data transmission, respectively. The energy available to S and R nodes at the start of each transmission slot can be written as

$$E_{ava,s}(i_{j,s}) = \begin{cases} E_{h,s}(i_{j,s}) + E_{ava,s}(N_{j-1,s}), & i_{j,s} = 1_{j,s}, \\ E_{ava,s}((i-1)_{j,s}) - E_{tx,s}(\tau_x((i-1)_{j,s})) - \delta((i-1)_{j,s}), & i_{j,s} > 1_{j,s}, \end{cases} \quad (3)$$

$$E_{ava,r}(i_{j,r}) = \begin{cases} E_{h,r}(i_{j,r}) + E_{ava,r}(N_{j-1,r}), & i_{j,r} = 2_{j,r}, \\ E_{ava,r}((i-1)_{j,r}) - E_{tx,r}(\tau_x((i-1)_{j,r})) + \alpha\delta((i-1)_{j,r}), & i_{j,r} > 2_{j,r}, \end{cases} \quad (4)$$

where, $E_{tx,s}(\tau_x((i-1)_{j,s}))$ and $E_{tx,r}(\tau_x((i-1)_{j,r}))$ is the amount of energy consumed by the S and R node in $(i-1)$ -th transmission slot of length τ at rate x ($x \in \{x_1 = 250 \text{ kbps}, \text{ and } x_2 = 1 \text{ Mbps}\}$), during j -th EH interval. The transmission power of S node in slot i is represented by $P_{tx,s}(\tau_x(i_{j,s}))$, where as the transmission power of $R \rightarrow D_1$ and $R \rightarrow D_2$ is denoted by $P_{tx,r}(\tau_x(i_{j,r}))$ and $P_{tx,r}(\tau_x(i'_{j,r}))$, respectively. The values of $P_{tx,s}(\tau_x(i_{j,s}))$, $P_{tx,r}(\tau_x(i_{j,r}))$ and $P_{tx,r}(\tau_x(i'_{j,r}))$ can be calculated as follows:

$$P_{tx}(\tau_x(i_j)) = \frac{N_0 W}{h} \left(2^{x(i_j)/W} - 1 \right), \quad (5)$$

where, N_0 is the noise spectral density, x is the rate and W is the channel bandwidth. From Figure 1(a) we can see that the energy buffer of R node have three different types of energies. Red lines represent

energy being transferred from the source, yellow lines represent harvested and black lines show the energy available from the previous interval.

Energy constraint. The maximum available energy for transmission is upper bounded by the maximum battery capacity. At any slot i_j the energies of S and R nodes are bounded by

$$0 \leq E_{\text{ava},s}(i_{j,s}) \leq E_{s,\text{max}}, \tag{6}$$

$$0 \leq E_{\text{ava},r}(i_{j,r}) \leq E_{r,\text{max}}. \tag{7}$$

Data buffer constraint. As mentioned before, the R node consists of finite size forwarding data buffer. This puts an additional constraint on the data transmission from $S \rightarrow R$. Therefore, the data to be transmitted should not exceed the buffer size for reliable communication. In addition to that, data causality constraint implies that the data cannot be transmitted before its arrival [19]. This constraint can be expressed as

$$0 \leq \sum_{i_{j,s} \in i_j} \tau_x(i_{j,s})x(i_{j,s}) - \sum_{i_{j,r} \in i_j} \tau_x(i_{j,r})x(i_{j,r}) \leq \text{BC}_{r,\text{max}}. \tag{8}$$

It is also evident from the above constraint that the buffer capacity acts as bottleneck for the S data packet size. Let BC_{r,i_j} be the buffer capacity at slot i_j and Z is the size of the data packet, then under the assumption

$$P_{\text{tx},s}(\tau_x(i_{j,s})) = 0 \quad \text{for } \text{BC}_{r,\text{max}} - \text{BC}_{r,i_j,r} < Z. \tag{9}$$

With all the constraints mentioned in Eqs. (6)–(9), the network throughput problem can be formulated as follows:

$$\rho_{\text{net}} = \rho_{s,d_1} + \rho_{r,d_2}, \tag{10}$$

where, ρ_{s,d_1} and ρ_{r,d_2} is the throughput achieved from $S \rightarrow D_1$ and $R \rightarrow D_2$, respectively. If M_s is the total amount of S data then the effective throughput from $S \rightarrow D_1$ is given as

$$\rho_{s,d_1} = \frac{M_s}{T} = \frac{M_s}{\sum_{j=1}^L (\sum_{i_{j,s}=1}^{N_j} \tau_x(i_{j,s}) + \sum_{i_{j,r}=2}^{N_j} \tau_x(i_{j,r}) + \Delta(j))}, \tag{11}$$

where, $\Delta(j)$ is the delay. If the available energy at a transmitting node is less than what is required for a successful transmission, the network nodes will wait for next EH interval to make their transmission successful. This wait time is called delay, denoted by Δ , shown in Figure 2. For the assumed system model, the R node being opportunistic does not suffer any delay for its own data. The total delay suffered by S node is given by the following equation:

$$\Delta = \sum_{j=1}^L \left(l(j) - \sum_{i_{j,s}}^{N_j} \tau_x(i_{j,s}) - \sum_{i_{j,r}}^{N_j} \tau_x(i_{j,r}) + \sum_{i'_{j,r}}^{N_j} \tau_x(i'_{j,r}) \right). \tag{12}$$

If M_r is the total amount of the R data then the effective throughput from $R \rightarrow D_2$ is given as

$$\rho_{r,d_2} = \frac{\sum_{j=1}^L \sum_{i'_{j,r} \in i_j}^{N_j} x(i'_{j,r})\tau_x(i'_{j,r})}{\sum_{j=1}^L (\sum_{i_{j,s}=1}^{N_j} \tau_x(i_{j,s}) + \sum_{i_{j,r}=2}^{N_j} \tau_x(i_{j,r}) + \Delta(j))}. \tag{13}$$

Using Eqs. (7)–(9) the objective function can be expressed as

$$\begin{aligned} & \arg \max_{x(i_j) \in \{x_1, x_2\}} \{ \mathbb{E} [\rho_{\text{net}}] \}, \\ & \text{s.t.} \quad 0 \leq E_{\text{ava},r}(i_{j,r}) \leq E_{r,\text{max}}, \\ & \quad P_{\text{tx},s}(\tau_x(i_{j,s})) = 0 \quad \text{for } \text{BC}_{r,\text{max}} - \text{BC}_{r,i_j,r} < Z, \\ & \quad 0 \leq \sum_{i_{j,s} \in i_j} \tau_x(i_{j,s})x(i_{j,s}) - \sum_{i_{j,r} \in i_j} \tau_x(i_{j,r})x(i_{j,r}) \leq \text{BC}_{r,\text{max}}. \end{aligned} \tag{14}$$

The computational complexity to solve the above objective function optimally increases exponentially with the number of EH intervals [20]. Conventional sub-optimal solution such as MDP [17] are also computationally expensive. Therefore, in the following we propose a JRPAP based on existing heuristics and intuitive allocation policies [12, 19]. In addition, a practical upper bound based on single step offline energy arrival has also been presented in Subsection 4.3.

3 Power allocation policies

This section presents three power allocation policies from the existing literature [12, 19] and applies it to the system model given in Section 2.

3.1 Generous power allocation (GPA)

In optimal transmission policy [19] assuming an offline EH arrival profile, the transmission rate increases in time and remains constant within an EH interval. Furthermore, whenever the transmission rate changes the energy consumed upto that instance is equal to the energy harvested upto that instance with no constraint on maximum battery size. Inspired by the optimal transmission policy, GPA for the proposed system model is presented. Therefore, with realistic constraints such as online EH profile and finite battery capacity the opportunistic R node will allocate power such that $R \rightarrow D_1$ transmission occurs at the maximum possible rate. This maximum possible rate can be calculated from $E_{\text{ava},r}(i_{j,r})$, and the transmission power required for 250 kbps and 1 Mbps. After $R \rightarrow D_1$ transmission, the remaining power is assigned to opportunistic $R \rightarrow D_2$ transmission.

3.2 Equal power allocation (EPA)

In equal power allocation [12], the R node will equally divide the total power available among all the relaying transmissions. However, for comparison purpose the EPA is modified such that the R node equally divides the total available power for $R \rightarrow D_1$ and $R \rightarrow D_2$ transmission. Depending upon the EH profile, this power allocation can lead to scenarios in which neither $R \rightarrow D_1$ nor $R \rightarrow D_2$ transmission is possible. The R node has to wait for next EH interval to make the $R \rightarrow D_1$ transmission. In the next EH interval, instead of splitting the energy, all the available energy is assigned to $R \rightarrow D_1$ transmission in order to avoid delay.

3.3 Transfer power allocation (TPA)

In non cooperative individual transmission policy [12], the power harvested from the i -th source is used by the R node to forward its data to i -th destination. Therefore, for the proposed system model using TPA, the R node only allocates the transferred energy for $R \rightarrow D_1$ transmission. If the transferred energy is not enough for the S data, R node will wait for the next EH interval. In the next EH interval all the available energy is assigned to $R \rightarrow D_1$ transmission.

$$P_{\text{ava},r}(i_{j,r}) = \alpha \delta(i_{j,s}). \quad (15)$$

3.4 Proposed policy: joint rate and power allocation policy (JRPAP)

In a cooperative EHWSN, the network performance is directly linked to resource allocation such as power assignment made at the R node. To achieve desirable network throughput is a challenging problem in scenarios where the R node also has its own data to transmit. In such a network, power assignment should be made such that both the nodes get a chance to transmit data in order to improve network throughput and satisfy the delay, energy and data buffer constraint. Different power allocation policies based upon the proposed system model are discussed above. However, in all the above mentioned policies the throughput of either $S \rightarrow D_1$ or $R \rightarrow D_2$ is compromised due to the power distribution made at the R node. For example, if EPA is used then there are chances that no transmission at R node can occur,

Algorithm 1 Joint rate and power allocation policy

Input: $x_1=250$ kbps, $x_2=1$ Mbps, $E_{\text{ava},r}(i_j,r)$, $P_{\text{req}}(\tau_x(i_j,r)) = P_{\text{tx}}(\tau_x(i_j))$, $\tau_x(i_j,r)$, $P_{\text{ava},r}(i_j,r) = \frac{E_{\text{ava},r}(i_j,r)}{\tau_x(i_j,r)}$, $E_{r,\text{max}}$, L .

```

1: for  $j = 1$  to  $L$  do
2:    $E_{\text{ava},r}(i_j,r) = E_{\text{ava},r}(i_j,r) + E_{h,r}(i_j,r)$ ;
3:    $E_{\text{ava},r}(i_j,r) = \min(E_{\text{ava},r}(i_j,r), E_{r,\text{max}})$ ;
4:   if  $P_{\text{ava},r}(i_j,r) \geq P_{\text{req}}(\tau_{x2}(i_j,r))$  then
5:     if  $P_{\text{ava},r}(i_j,r) \geq 2P_{\text{req}}(\tau_{x2}(i_j,r))$  then
6:        $P_{\text{ava},r}(i'_j,r) = P_{\text{ava},r}(i_j,r) - P_{\text{req}}(\tau_{x2}(i_j,r))$ ;
7:     else
8:        $P_{\text{ava},r}(i_j,r) = P_{\text{ava},r}(i'_j,r) = \frac{P_{\text{ava},r}(i_j,r)}{2}$ ;
9:       if  $P_{\text{ava},r}(i_j,r) \leq P_{\text{req}}(\tau_{x2}(i_j,r))$  then
10:        if  $P_{\text{ava},r}(i_j,r) \geq P_{\text{req}}(\tau_{x1}(i_j,r))$  then
11:           $P_{\text{ava},r}(i'_j,r) = P_{\text{ava},r}(i_j,r) - P_{\text{req}}(\tau_{x1}(i_j,r))$ ;
12:        else
13:          Wait for next energy harvesting interval;
14:          Goto  $E_{\text{ava},r}(i_j,r)$ ;
15:        end if
16:      end if
17:    end if
18:  else if  $P_{\text{ava},r}(i_j,r) \geq P_{\text{req}}(\tau_{x1}(i_j,r))$  then
19:     $P_{\text{ava},r}(i'_j,r) = P_{\text{ava},r}(i_j,r) - P_{\text{req}}(\tau_{x1}(i_j,r))$ ;
20:  else
21:    Wait for next energy harvesting interval;
22:    Goto  $E_{\text{ava},r}(i_j,r)$ ;
23:  end if
24: end for

```

Output: Calculate throughput based on the selected rate and power allocation.

if EH level is less than twice the energy required for transmission at 250 kbps. However, this may not be the case in GPA as it is more tilted towards the source data. TPA suffers from low power efficiency and thus low throughput. In addition, the intermittent nature of the EH process makes it difficult to use a specific power allocation policy for the complete transmission. Therefore, to cater for random energy arrivals it is necessary to use a joint rate and power allocation that can achieve a better overall network throughput.

In this paper, we propose a JRPAP which is given in Algorithm 1. In this policy, decision at the R node is formulated to act in the best interest of $R \rightarrow D_1$ and $R \rightarrow D_2$ transmission. Once the data and energy from the S node arrives at relay, it has to dynamically decide the rate and allocate power for the $R \rightarrow D_1$ transmission. The R node will first select transmission rate to be used for $R \rightarrow D_1$ transmission. For instance if rate $x_2 = 1$ Mbps is selected for data transmission, the node will check if the available power is twice the amount of the power required (calculated using Eq. (5)) for $R \rightarrow D_1$ transmission. Checking this condition ensures that enough energy will be available to opportunistically transmit data even after $R \rightarrow D_1$ transmission at highest rate possible. Therefore, during a transmission slot where this condition is satisfied, the R node will assign the required power, $P_{\text{req}}(\tau_{x_2}(i_j,r))$ for $R \rightarrow D_1$ transmission. In the next transmission slot, using the remaining power the R node will opportunistically transmit its data $R \rightarrow D_2$. In scenarios, where at the start of a transmission the amount of power available at the R node is between $P_{\text{req}}(\tau_{x_2}(i_j,r))$ and twice $P_{\text{req}}(\tau_{x_2}(i_j,r))$, the R node will be reluctant in allocating all its available power to $R \rightarrow D_1$ transmission. The R node is justified for this behavior because if it assigns all the available power for $R \rightarrow D_1$ transmission then there might be a case where little or no energy remains for $R \rightarrow D_2$ transmission. Therefore, in order to avoid the energy depletion state, the R node will prefer to allocate half of its available energy for $R \rightarrow D_1$ transmission and the remaining half for its own transmission $R \rightarrow D_2$. Once the power is equally divided, the data from $R \rightarrow D_1$ and $R \rightarrow D_2$ is transmitted at 250 kbps.

However, if the rate $x_1 = 250$ kbps is selected for data transmission, the R node will assign $P_{\text{req}}(\tau_{x_1}(i_j,r))$ for $R \rightarrow D_1$ and the remaining energy will be used for $R \rightarrow D_2$ transmission. In an EH interval where the available energy is below $P_{\text{req}}(\tau_{x_1}(i_j,r))$ no transmission is possible and the R

Table 1 Simulation parameters

Name and variable	Value
Length of EH interval l	12.5 ms
Energy transfer efficiency α	0.2
Data rates ρ [22]	250 kbps and 1 Mbps
Max buffer capacity $BC_{r,\max}$	500–1100 bits
Data length D_s	20000 bits
Bandwidth W	1 MHz
Noise spectral density N_0	10^{-19} W/Hz
$h_{r,s}$, h_{r,d_1} & h_{r,d_2}	-110 dB
$E_{r,\max}$ and $E_{s,\max}$	15 μ J

node will have to wait for the next EH instance. We envisioned that this intelligent decision making based on available power at the R node, ensures both the transmissions. This in turn will be able to achieve fairness in terms of throughput. Since our metric of interest is throughput we apply Jain's fairness index [21] which is given by the following formula:

$$F(\rho_{s,d_1}, \rho_{r,d_2}) = \frac{(\rho_{s,d_1} + \rho_{r,d_2})^2}{2(\rho_{s,d_1}^2 + \rho_{r,d_2}^2)}. \quad (16)$$

4 Simulation results

This section presents a comparison of GPA, EPA, TPA, and the proposed JRPAP in terms of network throughput, energy efficiency, delay, transmission time and fairness. The system parameters used are listed in Table 1. The EH profile used follows a uniform distribution with $E_{\text{mean}} = 5 \times 10^{-6}$ μ J and 1×10^{-6} μ J for S and R nodes, respectively. For simplicity, the size of S node packet, denoted by Z is always taken equal to BC_{r,i_j} .

4.1 JRPAP results

Figure 3 shows the comparison of network throughput ρ achieved by all the power policies for different sizes of R node buffer. It is evident from the figure that for all the policies throughput increases as the buffer size increases. JRPAP achieves throughput gain of 11%, 12% and 30% at buffer length of 1100 (bits) over policies GPA, EPA and TPA, respectively. At lower buffer size, the EPA and GPA have approximately the same throughput. At higher buffer size GPA throughput is slightly high. Since GPA is pro source, it allocates majority chunk of energy to $R \rightarrow D_1$. However, at times using EPA can result in energy allocation which can starve both $R \rightarrow D_1$ and $R \rightarrow D_2$ transmission.

Figure 4 shows the amount of time spent by each policy to transmit complete source data ($S \rightarrow R \rightarrow D_1$). This transmission time includes the total time spent by S and R nodes and the delays suffered due to opportunistic transmission and/or unavailability of energy. From Figures 3 and 4 it can be observed that for almost the same amount of transmission time, JRPAP outperforms EPA and GPA. The delay suffered by source data ($S \rightarrow R \rightarrow D_1$) is demonstrated in Figure 5. With increasing buffer size the amount of energy spent per packet also increases, this results in less amount of energy available for opportunistic data transmission and thus the delay due to it decreases.

The network energy consumption shown in Figure 6 includes both the energy consumed at S and R nodes for complete transmission of source data (T sec). It is evident from the results that with the increase in buffer size the energy consumption decreases as the number of packets required to transmit a fixed amount of source data decreases. The energy consumption of TPA is relatively high as compared to other three policies which is due to its biased nature that allows more transmission opportunities to $R \rightarrow D_2$.

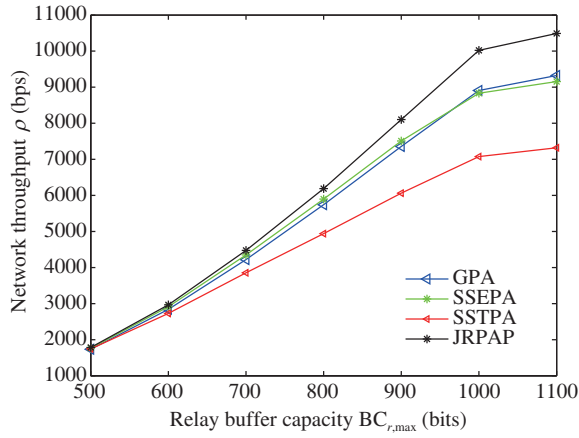


Figure 3 (Color online) Network throughput vs. relay buffer capacity.

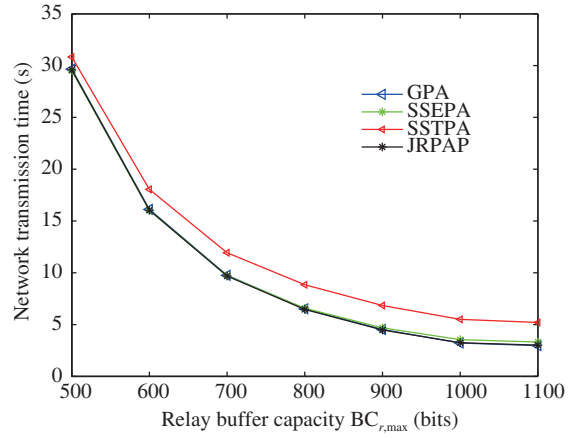


Figure 4 (Color online) Transmission time vs. relay buffer capacity.

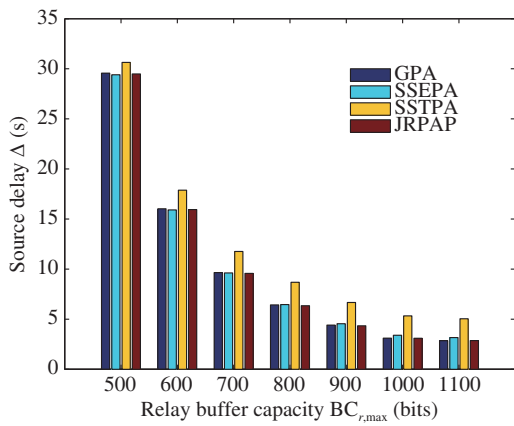


Figure 5 (Color online) Source delay vs. relay buffer capacity.

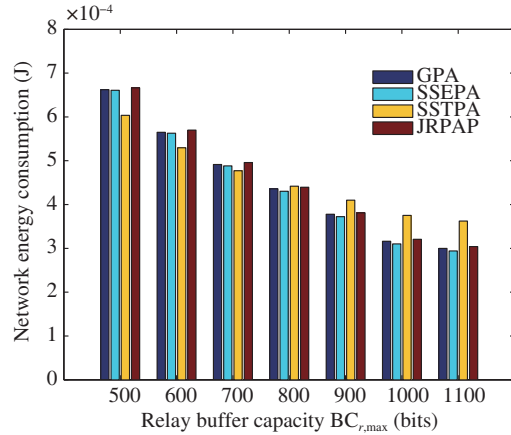


Figure 6 (Color online) Network energy consumption vs. relay buffer capacity.

In Figure 7, the comparison of no energy cooperation and energy cooperation is presented. It also shows the impact of energy transfer efficiency α on achievable throughput at buffer size 1100 bits. It is evident from the figure that throughput increases as the value of α increases from 0, that is no energy cooperation, to 1. More specifically, an increase of 2% and 8% is observed at $\alpha = 0.2$ and 1, respectively for JRPAP.

Fairness in terms of network throughput for each policy is shown in Figure 8. Fairness decreases with the increase in buffer size. This is due to increase in per packet energy consumption for $R \rightarrow D_1$ and lesser opportunities for $R \rightarrow D_2$. TPA achieves maximum fairness of 0.96 at buffer size of 1100 bits by compromising achievable throughput by approximately 30% compared to JRPAP. JRPAP on the other hand achieves 0.89 fairness while maintaining high throughput gains.

4.2 Throughput analysis using different channel conditions

In order to analyze the impact of channel variation, throughput performance of AWGN channel (with constant pathloss) and Rayleigh fading channel are compared. From Figure 9, it is evident that when AWGN channel is considered, the achievable throughput is maximum. For this system model, throughput of AWGN channel acts as the upper bound. However, the throughput achieved for the second scenario where it is assumed that the receiver side information (the power is adjusted according to the channel

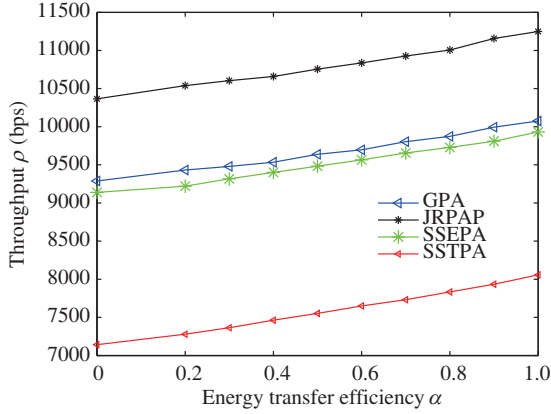


Figure 7 (Color online) Network throughput vs. energy transfer efficiency.

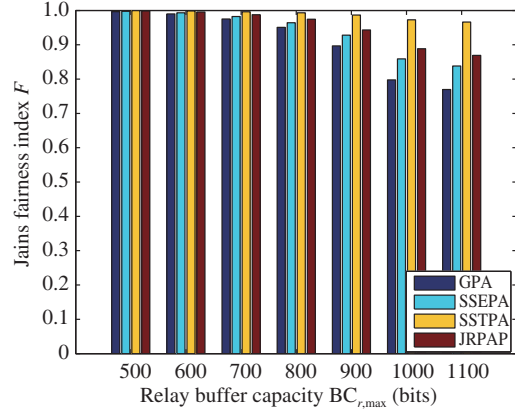


Figure 8 (Color online) Throughput fairness vs. relay buffer capacity.

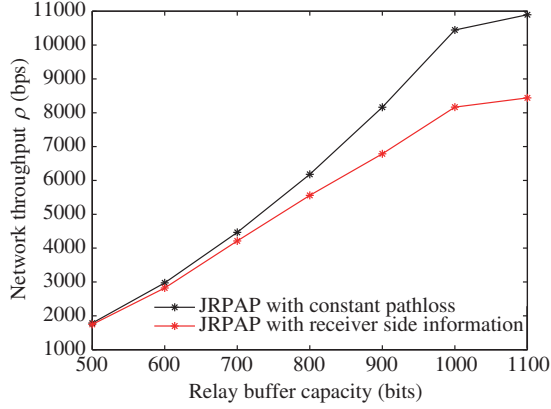


Figure 9 (Color online) Network throughput vs. relay buffer capacity.

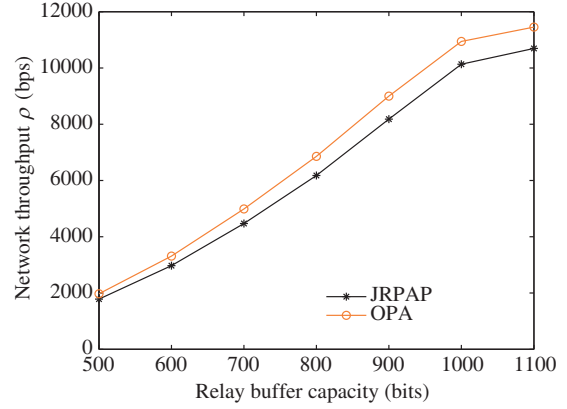


Figure 10 (Color online) Network throughput vs. relay buffer capacity.

gain) is available at the transmitter, is relatively low than the simple AWGN channel. In addition, the throughput will degrade further without any information about the receiver side channel conditions.

4.3 Performance upper bound

The optimal solution of the objective function presented in (14) requires offline knowledge of all the energy arrivals. Such a solution is of little practical value as the computational complexity associated with it will be very high, as often found in the case of dynamic programming [23]. This makes it difficult to implement in EHWSNs. To provide a practical upper bound, we assume an offline knowledge of only the next energy arrival. This knowledge can be practically achieved through energy forecasting [24]. Figure 10 shows that tailoring joint rate and power allocation policy serves as performance upper bound for JRPAP. This scheme is called offline power allocation (OPA) policy. In OPA, the transmitting node has information about the current and following EH instance. Using this information, the R node assigns transmission rate for the current slot such that there is enough remaining energy to support data transmission in the next transmission slots. Figure 10 shows that OPA achieves higher throughput than JRPAP. There is no significant difference between OPA and JRPAP at lower buffer sizes, mainly due to small energy expenditure of transmitting packets. However, at large buffer sizes OPA provides a much better throughput as packet transmission energy is comparatively high and the knowledge of next EH instance helps in scheduling packets and managing residual energy. Although not shown here, the throughput further increases as the knowledge of more EH instances is incorporated.

4.4 Joint rate and power allocation policy with energy and data aggregation (JRPAP-EDA)

From the results of Figure 3 it can be concluded the throughput achieved by all policies including JRPAP at smaller buffer sizes is relatively low. However, at higher buffer sizes significant gain in term of throughput is achieved by JRPAP. This necessitates the need of data aggregation (DA) [25]. Since the forwarding buffer size for the S node data is fixed, we only consider the DA on the relay's opportunistic data. To the best of our knowledge, the DA for an opportunistic scenario has not been considered before. This policy is called JRPAP-DA and it allows transmission of the aggregated data when maximum allowable packet size is reached. This aggregated data is transmitted based on the procedures defined in JRPAP.

Since EHWSN is energy-constrained, we also introduce the notion of energy aggregation (EA) for relay's opportunistic packets. To the best of our knowledge, this has also not been studied before. It is envisioned that using EA for successful transmission of aggregated data can increase opportunistic transmissions of the R node, thus increasing the overall network throughput. This variation is called JRPAP-EDA. In this policy, similar to JRPAP-DA the relay opportunistic data is aggregated till it satisfies the maximum allowable packet size [22]. Furthermore, energy for opportunistic data is also aggregated for successful transmission of this aggregated packet at the highest supportable rate. Thus, over coming the chance of energy overflow due to finite energy buffer. The JRPAP-EDA policy simplifies to JRPAP-EA when relay's opportunistic packet size is similar in size to the source packet. In this scenario, no DA will take place as it is assumed that relay's opportunistic data is always available. In addition, if the energy available for $R \rightarrow D_2$ transmission is less than what is required for 250 kbps, the residual energy is reserved for opportunistic data. It is further combined with the residual energy of the next EH interval to facilitate opportunistic transmission.

A throughput comparison between the three policies and JRPAP is shown in Figure 11. From the result, it is evident that using EA results in throughput gain at higher buffer sizes as compared to JRPAP, whereas, a gain in throughput at lower buffer sizes is observed when DA is used. This DA gain is due to availability of higher residual energy for the aggregated opportunistic data at lower buffer sizes. The gain in EA at higher buffer sizes is mainly due to the reservation of the residual energy for opportunistic transmissions. As shown in Figure 11, a combination of both EA and DA, JRPAP-EDA with 127 byte relay packet, can give throughput gains at all the buffer sizes.

In the following, we compare energy, delay and fairness results of JRPAP with JRPAP-EDA where the $R \rightarrow D_2$ data packet sizes for JRPAP-EDA are 37 and 127 bytes. The delay suffered by the source data ($S \rightarrow R \rightarrow D_1$) using JRPAP-EDA is shown in Figure 12. The delay of JRPAP-EDA with 127 bytes relay packet, at small buffer size is highest, whereas, the delay of JRPAP-EDA with 37 bytes relay packet is the lowest. This is because, JRPAP-EDA with 127 bytes relay packet leaves less residual energy for forwarding the source packet. Furthermore, as the buffer size increases the delay value of JRPAP-EDA with 127 bytes relay packet is almost comparable to JRPAP because at higher buffer sizes the source packet size reaches the DA limit. Figure 13 shows that the R node has to spend more energy in order to achieve high throughput using JRPAP-EDA with 127 bytes.

Figure 14 shows that fairness of JRPAP-EDA with 127 bytes relay packet initially increases, however, as the buffer size is increased this trend changes. The initial trend is mainly due to an increase in packet size of $R \rightarrow D_1$ transmission. It can be seen that the fairness of JRPAP-EDA with 127 bytes relay packet peaks at 800 bits (100 bytes) buffer size which is less than the size of DA limit, 127 bytes. The mismatch in packet size is equated by the priority of $R \rightarrow D_1$ transmission, resulting in same throughput. A decrease in fairness is observed as the packet size increases beyond 800 bits this is because the energy requirement increases for the $R \rightarrow D_1$ transmission thus decreasing the transmission opportunity of the $R \rightarrow D_2$ transmission. Even though fairness of JRPAP-EDA with 127 bytes relay packet decreases beyond 800 bits it still depicts highest fairness compared to JRPAP and JRPAP-EDA with 37 bytes relay packet mainly because of EA (as evident from the Figure 11). JRPAP-EDA with 37 bytes relay packet has the lowest fairness due the fact that the throughput for $S \rightarrow D_1$ dominates with the increasing buffer

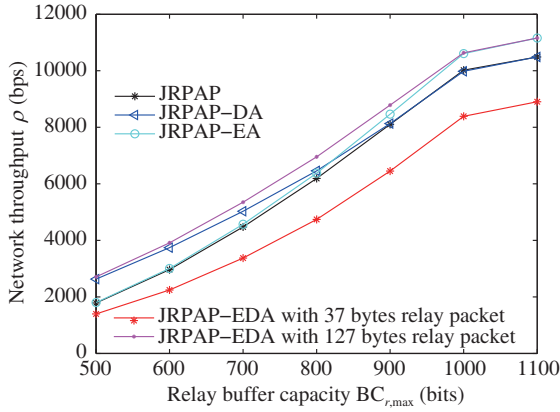


Figure 11 (Color online) Network throughput vs. energy transfer efficiency.

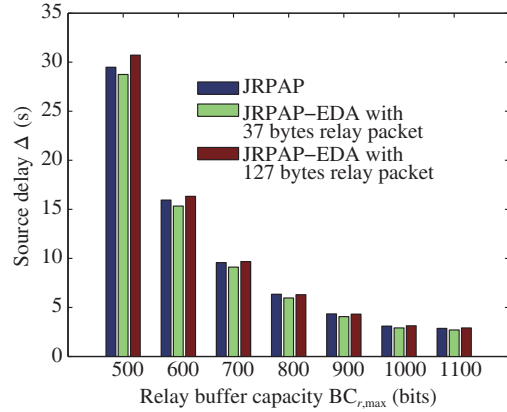


Figure 12 (Color online) Source delay vs. relay buffer capacity.

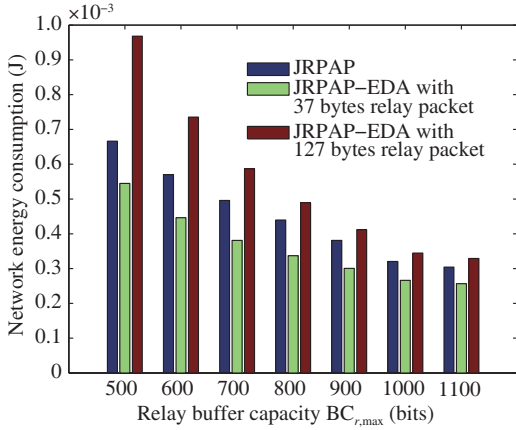


Figure 13 (Color online) Network energy consumption vs. relay buffer capacity.

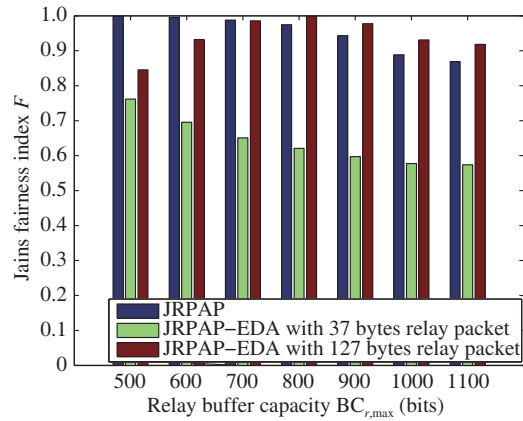


Figure 14 (Color online) Throughput fairness vs. relay buffer capacity.

size. Furthermore, using Figures 11–14 it can be observed that JRPAP-EDA with 127 bytes relay packet achieves highest throughput and comparable fairness at a cost of relatively high energy consumption and delay for the source data.

5 Conclusion

This paper presents a unified energy and data cooperation model in a cooperative EHWSN with an opportunistic relay. By applying different intuitive power allocation policies at the relay such as GPA, EPA and TPA, throughput, fairness, delay, energy and transmission time of EHWSN are studied under data and energy causality constraints. The results show that for the above policies and given EH profile, increasing the data buffer size causes a decrease in energy consumption, delay and transmission time as it curtails relay’s opportunistic behavior and compromises its throughput. The results show that GPA achieves highest throughput, whereas, TPA provides highest fairness. Specifically no single intuitive policy stands out in terms of all the performance parameters, therefore, a novel and opportunistic power allocation policy named JRPAP at the relay is proposed. It performs significantly better than the intuitive policies and maintains a balance between the performance matrix of EHWSNs. A throughput gain of 30% is observed over TPA which using JRPAP. JRPAP also achieves a comparable fairness of 0.89 against 0.96 of TPA. In all the policies, since, there is no significant throughput gain at lower buffer sizes, therefore, a modified version of JRPAP, JRPAP-EDA is proposed which combines both EA and DA for relay’s opportunistic data. JRPAP-EDA with 127 bytes relay packet depicts network throughput gain at all

buffer sizes over JRPAP, JRPAP-EA and JRPAP-DA. In essence relay buffer capacity is a key factor in determining the trade offs that exist between energy consumption, source delay and fairness. In addition, an optimal buffer size for $R \rightarrow D_1$ transmission exists which can provide ideal fairness. The future work is focused on determining the optimal buffer capacity for overall performance improvement in EHWSNs.

References

- 1 Kausar A Z, Reza A W, Saleh M U, et al. Energizing wireless sensor networks by energy harvesting systems: scopes, challenges and approaches. *Renew Sustain Energy Rev*, 2014, 38: 973–989
- 2 Huang C, Zhang R, Cui S G. Throughput Maximization for the Gaussian Relay Channel with energy harvesting constraints. *IEEE J Sel Areas Commun*, 2013, 31: 1469–1479
- 3 Luo Y, Zhang J, Letaief K B. Throughput maximization for two-hop energy harvesting communication systems. In: *Proceedings of IEEE International Conference on Communications*, Budapest, 2013. 4180–4184
- 4 Gunduz D, Devillers B. Two-hop communication with energy harvesting. In: *Proceedings of the 4th IEEE International Workshop on Computational Advances in Multi-Sensor Adaptive Processing (CAMSAP)*, San Juan, 2011. 201–204
- 5 Varan B, Yener A. The energy harvesting two-way decode and forward relay channel with stochastic data arrivals. In: *Proceedings of IEEE Global Conference on Signal and Information Processing*, Austin, 2013. 371–374
- 6 Varan B, Yener A. Energy harvesting two-way communications with limited energy and data storage. In: *Proceedings of the 48th Asilomar Conference on Signals, Systems and Computers*, Pacific Grove, 2014. 1671–1675
- 7 Gurakan B, Ozel O, Yang J, et al. Energy cooperation in energy harvesting communications. *IEEE Trans Commun*, 2013, 61: 4884–4898
- 8 Mitcheson P D. Alternative power sources for miniature and micro devices. In: *Proceedings of the 18th International Conference on Solid-State Sensors, Actuators and Microsystems*, Anchorage, 2015. 928–933
- 9 Lee D S, Liu Y H, Lin C R. A wireless sensor enabled by wireless power. *Sensors*, 2012, 12: 16116–16143
- 10 Lu X, Flint I, Niyato D, et al. Performance analysis of simultaneous wireless information and power transfer with ambient RF energy harvesting. In: *Proceedings of Wireless Communications and Networking Conference*, New Orleans, 2015
- 11 Guo S, He C, Yang Y. ResAll: energy efficiency maximization for wireless energy harvesting sensor networks. In: *Proceedings of the 12th Annual IEEE International Conference on Sensing, Communication, and Networking*, Seattle, 2015. 64–72
- 12 Ding Z, Perlaza S M, Esnaola I, et al. Power allocation strategies in energy harvesting wireless cooperative networks. *IEEE Trans Wirel Commun*, 2014, 13: 846–860
- 13 Nasir A A, Zhou X, Durrani S, et al. Wireless-powered relays in cooperative communications: time-switching relaying protocols and throughput analysis. *IEEE Trans Commun*, 2015, 63: 1607–1622
- 14 Biazon A, Zorzi M. Joint transmission and energy transfer policies for energy harvesting devices with finite batteries. *IEEE J Sel Areas Commun*, 2015, 33: 2626–2640
- 15 Baidas M W, Alsusa E A. Power allocation, relay selection and energy cooperation strategies in energy harvesting cooperative wireless networks. *Wirel Commun Mob Comput*, 2016, 16: 2065–2082
- 16 Afghah F, Razi A, Abedi A. Throughput optimization in relay networks using Markovian game theory. In: *Proceedings of Wireless Communication and Networking Conference (WCNC)*, Cancun, 2011. 1080–1085
- 17 Minasian A, ShahbazPanahi S, Adve R S. Energy harvesting cooperative communication systems. *IEEE Trans Wirel Commun*, 2014, 13: 6118–6131
- 18 Luo Y, Zhang J, Letaief K B. Optimal scheduling and power allocation for two-hop energy harvesting communication systems. *IEEE Trans Wirel Commun*, 2013, 12: 4729–4741
- 19 Yang J, Ulukus S. Optimal packet scheduling in an energy harvesting communication system. *IEEE Trans Commun*, 2012, 60: 220–230
- 20 Tutuncuoglu K, Yener A. Optimum transmission policies for battery limited energy harvesting nodes. *IEEE Trans Wirel Commun*, 2012, 11: 1180–1189
- 21 Jain R, Durrresi A, Babic G. Throughput fairness index: an explanation. 1999. http://www.cse.wustl.edu/~jain/atmf/ftp/af_fair.pdf
- 22 IEEE 802 Working Group. IEEE standard for local and metropolitan area networks—part 15.4: low-rate wireless personal area networks. *IEEE Std 802.15.4e*, 2011
- 23 Bellman R E, Dreyfus E S. *Applied Dynamic Programming*. Princeton: Princeton University Press, 2015
- 24 Cammarano A, Petrioli C, Spenza D. Pro-energy: a novel energy prediction model for solar and wind energy-harvesting wireless sensor networks. In: *Proceedings of the 9th International Conference on Mobile Ad-Hoc and Sensor Systems*, Las Vegas, 2012. 75–83
- 25 Krishnamachari L, Estrin D, Wicker S. The impact of data aggregation in wireless sensor networks. In: *Proceedings of the 22nd International Conference on Distributed Computing Systems Workshops*, Vienna, 2002. 575–578